

Formation and crystallization of bulk Pd₈₂Si₁₈ amorphous alloys^①

PU Jian(蒲建), WANG Jian-feng(王敬丰), XIAO Jian-zhong(肖建中), CUI Kun(崔昆)
(State Key Lab of Plastic forming Simulation and Die & Mould Technology,
Huazhong University of Science & Technology, Wuhan 430074, China)

Abstract: Bulk amorphous Pd₈₂Si₁₈ alloy with the largest diameter of 8 mm was prepared by water quenching the molten alloy with flux medium in a quartz tube. The calculation result indicates that the bulk Pd₈₂Si₁₈ amorphous alloys have a low critical cooling rate (R_c) of 4.589 K/s or less. The experimental results show that purifying melt may improve glass forming ability(GFA) of undercooled melt, while liquid phase separation (LPS) of undercooled melt will decrease its GFA. There are some differences in crystallization experiments between bulk metallic glass and amorphous ribbons of Pd₈₂Si₁₈ alloys. These include the numbers of exothermic peak, glass transition temperature T_g , crystallization temperature T_x , region of undercooling liquid ($\Delta T = T_x - T_g$) respectively. The links of cooling rates of melt and crystallization of Pd₈₂Si₁₈ amorphous alloys are explored.

Key words: bulk amorphous alloys; Pd₈₂Si₁₈; glass forming ability; undercooling; critical cooling rate

CLC number: TB 3

Document code: A

1 INTRODUCTION

Metallic glass is regarded as a state that is of disorder unlike crystal alloys with periodic atom structure. So it shows excellent capabilities of soft magnetism, mechanics, corrosion resistance, etc. However, most of amorphous alloys were produced by using rapid solidification methods such as splat quenching, melt spinning, and so on, with characteristic cooling rates of $10^4 - 10^6$ K/s. Because amorphous alloys are prepared with silk, powder and ribbon, it is greatly limited in engineering application. Recently, several bulk amorphous alloys with excellent glass forming ability(GFA) at cooling rate of 10^3 K/s or less have been developed such as Zr_{41.2}Ti_{13.8}Cu_{12.5}Ni_{12.5}Be_{22.5}^[1], Pd₄₁Ni₁₀Cu₂₈P₂₁ alloy^[2].

Perepezhko^[3] expounded a new idea on preparing bulk amorphous alloys: if nucleation process has been controlled, the melt can be undercooled below its glass transition temperature(T_g). Thus undercooled melt might form bulk amorphous alloys at slow cooling rate. Competition to glass formation arises from heterogeneous crystallization that started at melt inclusions such as oxides, and from homogeneous crystallization. Therefore all kinds of techniques have been developed to achieve homogeneous nucleation. Kui^[4] found heterogeneous nucleation may be hindered and high undercooling achieved in melts held in a molten flux or slag such as B₂O₃. Kui and co-workers^[5] formed spheres with about 7 mm in diameter of

Pd₄₀Ni₄₀P₂₀ bulk amorphous alloys at a low cooling rate of about 0.75 K/s.

Compared with conventional binary and ternary amorphous alloys, we report our study on formation of bulk amorphous Pd₈₂Si₁₈ alloy produced by water quenching the molten alloy together with flux medium in a quartz tube. Time-temperature-transformation (TTT) diagrams are used for estimating critical cooling rates R_c . The effect of undercooling and cooling rates of Pd₈₂Si₁₈ melt for the GFA is discussed. The links of cooling rates of melt and crystallization of Pd₈₂Si₁₈ amorphous alloys are also explored.

1 EXPERIMENTAL

Mixtures of elements of Pd(99.999%) and Si(99.99%) having nominal composition Pd₈₂Si₁₈ (in mole fraction, %) were alloyed by radio frequency (RF) induction melting under Ar atmosphere (99.999%). Ingots of typical size of 1.5 - 2.5 g were prepared.

In the experiments, a Pd₈₂Si₁₈ ingot coated by anhydrous B₂O₃ was put in a dry, cleaned fused silica tube. The system was then heated up to 1371 K ($T_m + 300$ K) and evacuated to about 10^{-1} Pa. Prolonged heat treatment was applied for about 4 h. Owing to thermal cycling treatment, the melts achieve a stable undercooling. Then the system was transferred to the furnace that was preset a stable temperature above T_m of Pd₈₂Si₁₈. The schematic diagram of the experimental setup is shown in Fig. 1. We may make melts

① Received date: 2002 - 11 - 11; Accepted date: 2003 - 02 - 08

Correspondence: XIAO Jian-zhong, Professor; Tel: + 86-27-87542800; E-mail: jzxiao@public.wh.hb.cn

crystallize in a designated undercooling by the way of presetting furnace temperature. The actual temperature of the molten specimen was read by a thermocouple that is sheathed by another fused silica tube and insert directly into the molten specimen. Cooling of the sample may be changed by air cooling, water quenching and salt water quenching and so on. Because flux may avoids oxidation from external environment and eliminates impurities from specimen, heterogeneous nuclei of melts may be greatly dissolved.

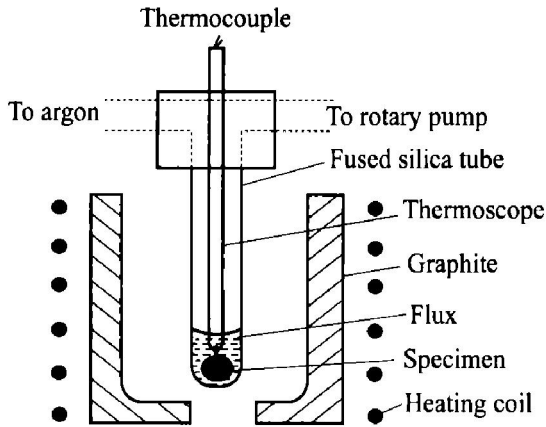


Fig. 1 Schematic of undercooling experiment

Finally, the specimen was cut by diamond saw, polished, and chemically etched. The etchant used was HCl:HNO₃:H₂O = 5:1:3 (by volume). Microstructural observation of different undercooled specimens were conducted by optical and scanning electron microscopy (SEM). The crystalline/amorphous nature of specimens were detected by X-ray diffraction (PHILIPS X'PERT MPD PRO), using CuK_α radiation. Crystallization of the amorphous specimen was studied using a Perkin-Elmer differential calorimeter (DSC-7).

2 RESULTS

According to Pd-Si binary phase diagram, at low undercooling, a representative microstructure is Pd₃Si dendrites, and the matrix consists Pd solution and Pd₃Si compound phase. It is obvious that Pd₃Si results from dendritic crystallization. Pd and Pd₃Si combine to form an eutecticlike structure. With the bulk supercooling increased, the microstructure of undercooled Pd₈₂Si₁₈ alloy specimen has been refined. When molten specimen is undercooled larger than 190 K below T_m , liquid phase separation of melts occurs. A SEM micrograph shown in Fig. 2(a) is displayed that solidification micrograph of melt is connected network with 282 K. This is because undercooled Pd-Si melt has separated into two different componential regions from one homogeneous liquid. Fig. 2(b) shows backscatter electron composition (BEC) micro-

graph. Considering from BEC imaging principle, it can be confirmed that bright regions are Pd-rich, whereas black regions are Si-rich. According to Gibbs phase rule, the final crystalline undercooled specimen should contain only two phases. However there are three phases, Pd, Pd₃Si and Pd₉Si₂ present in an undercooled specimen with undercooling larger than 190 K. Characteristic crystalline peaks of the metastable phase Pd₉Si₂ in the XRD is shown in Fig. 3(a). Guo^[6] predicted that the characteristic wavelength λ of a spinodal network decreases monotonically with undercooling of melt. It coincides with our experimental results, one with $\Delta T = 282$ K and $\lambda = 800$ nm, and the other with $\Delta T = 294$ K and $\lambda = 600$ nm. With undercooling of the melt increased, connected networks of melt are broken up into some liquid droplets with size in nanometer order induced by interfacial tension. Its solidification microstructure is displayed with 320 K in Fig. 2(c).

It is difficult that bulk Pd₈₂Si₁₈ amorphous alloys are directly formed by undercooled melt below T_g temperature because of the presence of impurities that act as heterogeneous crystal nuclei. Bulk Pd₈₂Si₁₈ amorphous alloy with the largest diameter of 8 mm is prepared by water quenching the molten alloy together with flux medium in a quartz tube. Fig. 3(b) shows the XRD pattern for the as-prepared bulk Pd₈₂Si₁₈ amorphous alloy with size of 8 mm. No peak corresponding to crystalline phase can be detected. This indicates that the sample is fully amorphous.

3 DISCUSSION

3.1 Evaluation of glass-forming ability (GFA) of bulk Pd₈₂Si₁₈ amorphous alloys

The classical theory of nucleation and growth of crystalline phases in an undercooled melt has been used to estimate the GFA of amorphous alloys. A high value of reduced glass transition temperature or a deep eutectic should favor glass formation^[7]. This prediction is in good agreement with observations on Pd₈₂Si₁₈ alloys. In order to evaluate the GFA of Pd₈₂Si₁₈ alloys, The model of the isothermal transformation involving nucleation and growth was chosen to construct TTT diagrams, which was proposed by Davies and later developed by Uhlmann^[8]. This model incorporated with kinetic and thermodynamic factors. The critical cooling rates of Pd₈₂Si₁₈ alloys will be calculated by its TTT diagrams. In order to obtain agreement with the experimentally observed low critical cooling rates, G^* is set to 60 kT for a reduced undercooling $\Delta T_r = (T_m - T)/T_m$ of 0.2. G^* corresponds to the energy barrier for nucleation in the kinetic formulation. If transform volume fraction $x = 10^{-6}$ of crystal solid is taken as solid as

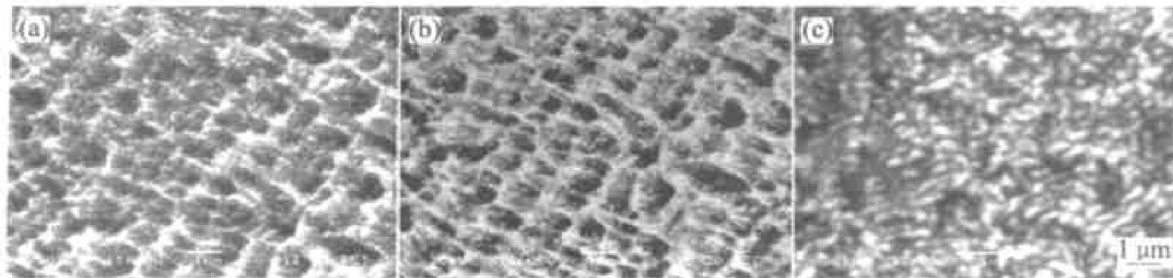


Fig. 2 SEM micrographs of Pd₈₂Si₁₈ alloy

(a) and (b) —Second electron image, Δ*T* = 282 K; (c) —Microstructure of undercooled specimen, Δ*T* = 320 K

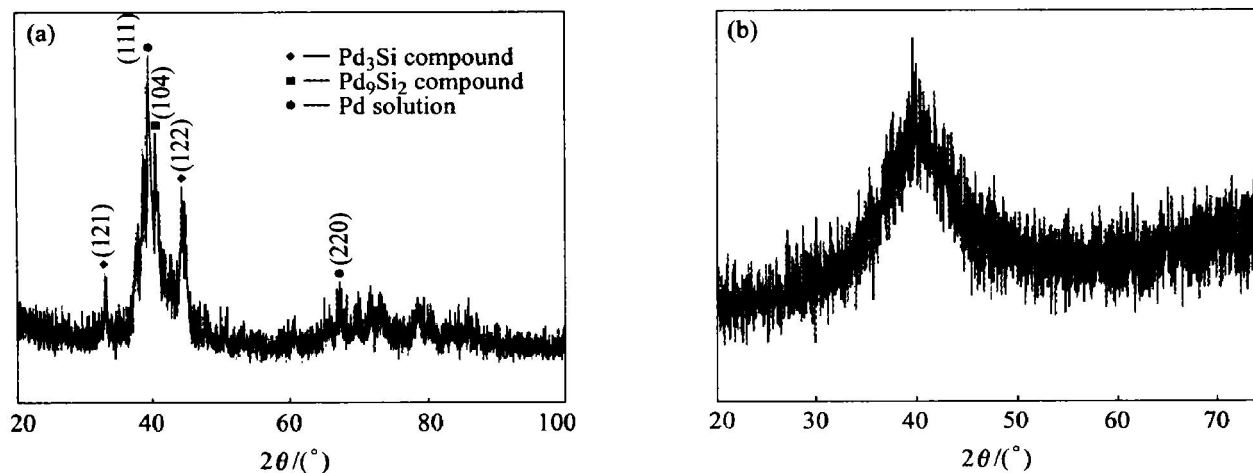


Fig. 3 X-ray diffraction patterns of Pd₈₂Si₁₈ alloys

(a) —Undercooling; (b) —Fluxing and water quenching

amorphous-crystal transformation. The TTT curve on critical cooling rates forming amorphous alloy can be calculated using the following equation :

$$t = \frac{9.3n}{kT} \left[\frac{a_0^3 x}{f^3 N_0} \frac{\exp\left(\frac{1.229}{T_r^3 \Delta T_r^2}\right)}{\left|1 - \exp\left(-\frac{\Delta H_m^f \Delta T_r}{RT_r T}\right)\right|^3} \right]^{\frac{1}{4}} \quad (1)$$

where *t* is time forming *x* of crystalline solid, η is the viscosity of melt, *a*₀ is an atomic diameter, *f* is a structure constant, *N*₀ is the number of atoms per unit volume, *k* is Boltzman constant, *R* is gas constant, *H*_m^f is fusion enthalpy per molar. The parameters have been taken in Table 1.

It is very difficult to measure experimentally the viscosity of supercooled liquid, but Tsang^[9] found capillary flow method may accurately measure viscosity of Pd₈₂Si₁₈ alloys.

The viscosity of undercooled Pd₈₂Si₁₈ melt be

Table 1 Values of parameters for calculation in Eqn. (1)

<i>T_m</i> /K	$\bar{a}_0/\text{Å}$	<i>N</i> ₀ /m ⁻³	<i>f</i>
1 071	4.127 2	6.424 × 10 ²⁸	1
<i>H_m^f</i> /(J•mol ⁻¹)	<i>k</i> /(J•K)	<i>R</i> /(J•mol ⁻¹ K ⁻¹)	
4 906.44	1.381 × 10 ⁻²³	8.31	

tween the liquidus temperature *T*_m and the glass transition temperature *T*_g can be described using Vogel-Fulcher expression:

$$\ln \eta = -3.779 + (1102.135 / (T - 684)) \quad (2)$$

The critical cooling rates *R*_c necessary for amorphous phase formation can be evaluated from TTT curve calculated using Eqn. (1) as shown in Fig. 4. *R*_c can be approximated as follows:

$$R_c = (T_m - T_n) / t_n \quad (3)$$

where *T*_n and *t*_n are the temperature and the time

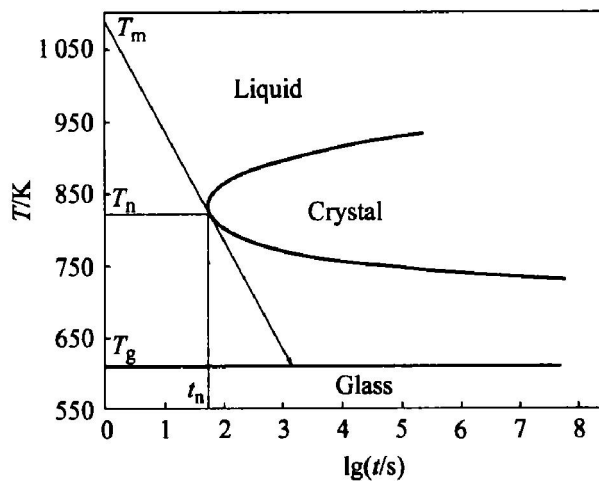


Fig. 4 Calculated TTT curve and the estimated critical cooling curve for Pd₈₂Si₁₈ alloy, *G*^{*} = 60 kT

at the nose of the TTT curve, respectively. Thus the R_c necessary for Pd₈₂Si₁₈ amorphous alloy is evaluated to be 4.589 K/s from Eqn. (3). Since the value is so small that the bulk Pd₈₂Si₁₈ amorphous alloys are possibly produced by air cooling on condition of homogeneous nucleation. But bulk Pd₈₂Si₁₈ amorphous alloys could not be prepared at a low critical cooling rates. This implies that homogeneous crystal nucleation dose not occur in experiments. Due to some effects of impurities of melts, heterogeneous energy barrier to nucleation changes from G_{het}^* to $G_{het}^* f(\theta)$. Here θ is the contact angle of the effective catalyst in a liquid, $f(\theta)$ is factor of the contact angle and is given by

$$f(\theta) = \frac{1}{4}(2 - 3\cos\theta + \cos^3\theta) \quad (4)$$

The more the θ , the less the $f(\theta)$ between heterogeneous nuclei and melt. When θ varies from 0° to 180°, the value of $f(\theta)$ is in a range from 0 to 1. In this case, homogeneous nucleation may come about, because heterogeneous nuclei are completely eliminated. Fig. 5 shows that the R_c of Pd₈₂Si₁₈ amorphous alloy will be decreased with $f(\theta)$ increased. Consequently preparing bulk Pd₈₂Si₁₈ amorphous alloys in the experiments need higher critical cooling rates than theory calculation, because impurities are unavoidable in an alloy melt. Therefore fluxing will provide useful tool in improving GFA of Pd₈₂Si₁₈ melts and reducing the R_c of bulk Pd₈₂Si₁₈ amorphous alloys.

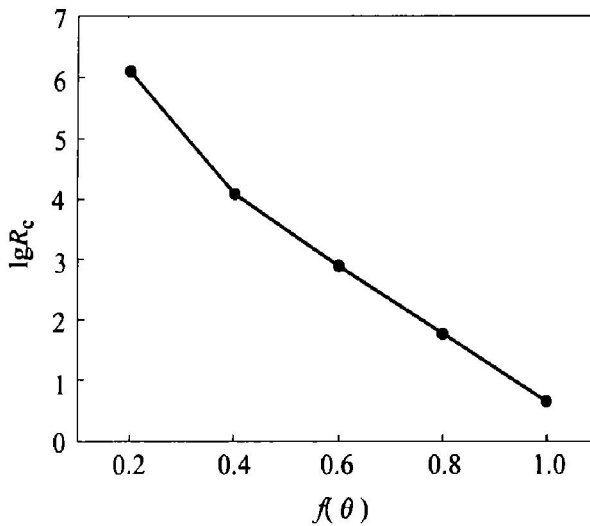


Fig. 5 Relations between critical cooling rates R_c and infiltration angle factor $f(\theta)$ of Pd₈₂Si₁₈ amorphous alloy

3.2 Effect of liquid phase separation(LPS) of undercooled Pd₈₂Si₁₈ melts for its GFA

Considering from thermodynamics point of view, the attraction between like species in an eutectic alloy is stronger than that between the unlike species, so the like species in the melt prefer to stay together. In eutectic system, when undercooled melt cool below its miscibility gap, LPS of melt will occur. Namely a

homogeneous liquid splits into multiple undercooled liquid networks intertwined with each other. There are two mechanisms for LPS, which are nucleation and growth (LNG) and spinodal decomposition (LSD)^[10].

When molten Pd₈₂Si₁₈ is undercooled to 190 K, the homogeneous liquid splits into two undercooled liquids. i. e., $L \rightarrow L_1 + L_2$, L_1 is Si-rich regions, but L_2 is Pd-rich regions. LPS of undercooled Pd₈₂Si₁₈ melts will affect its GFA from two aspects:

1) LPS of melts will provide driving force for crystallization of undercooled Pd₈₂Si₁₈ melts. Free energy curve of Pd₈₂Si₁₈ alloys in Fig. 6 shows C_0 composition of melt with an undercooled temperature cannot crystallize in thermodynamics, because it need to increase free energy ΔG_2 . But when a homogeneous original C_0 composition changes into two different liquid compositions C_1 and C_2 , undercooled melt will hold driving force of crystallization ΔG_1 in free energy. Thus the melt can start to crystallize in the undercooling. On another side, thinking of phase diagram of Pd-Si alloy, after LPS of melt occurs, comparing undercooling of C_0 , it is clear that undercooling of melt among C_1 and C_2 is the largest. And so driving force for crystallization of the undercooled liquid phase will be enhanced. Crystallization of the liquid phase results in nucleation in another liquid phase. Ultimately GFA of undercooled Pd₈₂Si₁₈ melts is diminished.

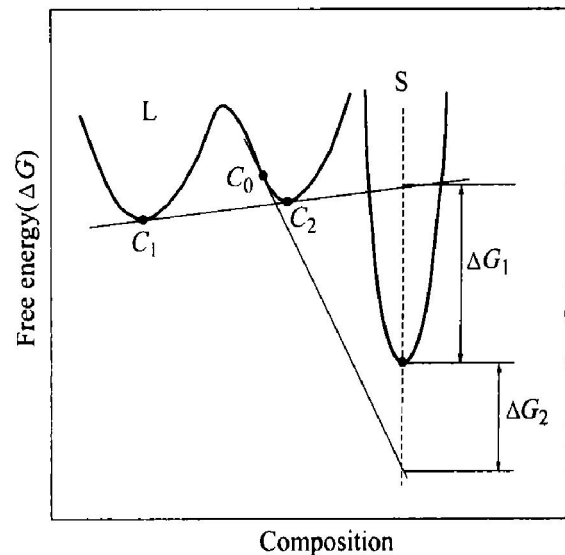


Fig. 6 Schematic diagram of free energy variety after liquid phase separation of Pd-Si melts

2) On account of formation of LPS of undercooled melt, there are a lot of interfaces between two liquid phases. Those interfaces may provide effective nucleation sites for nucleation of melt. It is a pity that currently no directly experimental evidences indicate nucleation between liquid interfaces. It is assumed that the interfacial energy may be too small to satisfy interfacial energy between crystalline and liquid. But

in the experiment of devitrification of amorphous ribbons $\text{Al}_{88}\text{Gd}_6\text{La}_2\text{Ni}_4$, it separates into the Al-rich and solute-rich amorphous regions, having typical wavelength $\lambda = 40$ nm. TEM studies reveal a preferential rapid nucleation of $\alpha\text{-Al}$ at the interface of phase-separated regions^[11].

Therefore, LPS in general does not favor the GFA of eutectic system. If spinodal microstructure of undercooled melt whose characteristic wavelength is very short can be “frozen” by rapid solidification, a spinodal metallic glass alloys will be formed^[12].

3.3 Crystallization of $\text{Pd}_{82}\text{Si}_{18}$ amorphous alloys

As the amorphous alloys are heated, the glass undergoing structural relaxation and internal equilibrium is approached. If the glass has been transformed to crystalline, some excellent properties of the materials will be debased. Hence high quality amorphous alloys require good thermal stability. The temperature interval $\Delta T = T_x - T_g$ is a measure of the thermal stability of the undercooled liquid (T_x is crystallization temperature). The DSC signal on heating a bulk $\text{Pd}_{82}\text{Si}_{18}$ amorphous alloys at 20 K/min which was prepared by fluxing and water quenching method is given in Fig. 7. The sample is protected by flowing argon (99.999%). T_{g1} , T_{x1} , T_{x2} and undercooling liquid region ($\Delta T = T_x - T_g$) of bulk $\text{Pd}_{82}\text{Si}_{18}$ amorphous alloys are 613, 632, 668 and 55 K respectively. The sample is not oxidized from environment in DSC experiments.

By investigating crystallization of Pd-Si amorphous ribbons, Masumoto and Maddin^[13] found that the glass experiences two metastable phase transformation and form stable Pd and Pd_3Si structure finally. Thermal effect from two metastable transformation was too small to detect by DSC instrument. Thus DSC curve of the sample has only

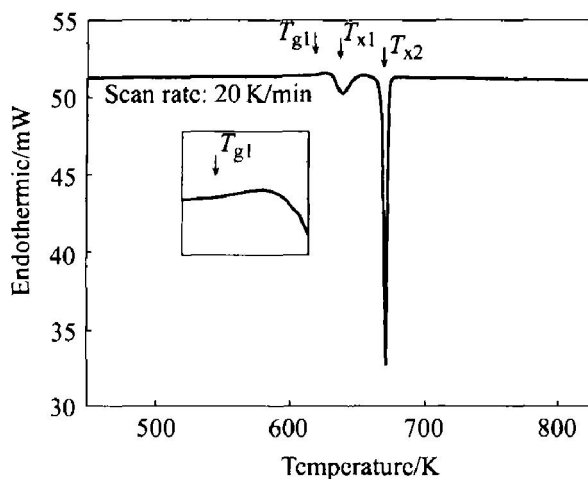


Fig. 7 DSC scan of bulk $\text{Pd}_{82}\text{Si}_{18}$ amorphous alloy taken at a heating rate of 20 K/min

single exothermic peak^[13]. Moreover, Nanao and Maeda indicated that if the samples is not oxidized in DSC experiment, Pd-Si amorphous ribbons did not undergo transition of metastable phase and directly form stable phase^[14].

However exothermic peaks of DSC curve become two in bulk $\text{Pd}_{82}\text{Si}_{18}$ amorphous alloys prepared at low cooling rates. We must study the reason why the difference appears between the two amorphous specimens. As undercooled melt transform to the glass, in order to suppress crystallization from undercooled melt, a metastable amorphous phase with phase separation character may be formed. Compared with “ideal” amorphous with completely disorder structure, the glass may possess several amorphous parts with different composition or “structure” in a sample. Amorphous alloys prepared by rapid solidification may go over metastable regions and preserve the structure of the liquid with higher disorder structure. Thus its crystallization shows eutectic crystallization character (single exothermic peak). Whereas crystallization of the bulk amorphous alloys shows that several amorphous parts crystallize respectively. Chen^[15] found that there are not enough time for liquid phase separation to take place in $\text{Pd}_{82}\text{Si}_{18}$ melt beyond cooling rate of about 1 000 K/s. In experiments, on account of thermal stability distinction of two amorphous parts, crystallization of the bulk glass presents two exothermic peaks. Intensity distinctness of two exothermic peaks may ascribe to volume fraction difference of two part amorphous alloys in a samples.

When compared to rapidly quenched glassy $\text{Pd}_{82}\text{Si}_{18}$ ribbons^[16], the present bulk glassy $\text{Pd}_{82}\text{Si}_{18}$ alloys have the following changes:

- 1) a lower glass transition temperature T_g , from 640 K to 613 K.
- 2) a higher crystallization temperature T_g , from 655 K to 668 K.
- 3) a wider region of undercooling liquid ΔT , from 15 K to 55 K.

Free energy of T_g temperature in the same sample is not almost change with difference of cooling rate of melt. Metallic glass prepared at a slower cooling rate should have a lower amount of free volume and Gibbs free energy. With the glass heated, it will be provided higher crystallization driving force than amorphous ribbons. So its structural relaxation may easily take place. This may explain the lower T_g in bulk amorphous alloys. Because melt flux decrease atomic oxygen and impurities, the removal of heteronucleants raises T_x . Since region of undercooling liquid ΔT of bulk metallic glass become wider, its thermal stability has been improved greatly.

4 CONCLUSIONS

1) Bulk amorphous Pd₈₂Si₁₈ alloy with the largest diameter of 8 mm was prepared by water quenching the molten alloy together with flux medium in a quartz tube with low cooling rates. A thermodynamic evaluation (Temperature-Time-Transformation diagrams) has been made by using the classical crystalline nucleation and growth theory to calculate critical cooling rates R_c of Pd₈₂Si₁₈ amorphous alloys. Calculation result shows the glass with very low R_c of 4.589 K/s as homogeneous nucleation occurs. Its R_c will be greatly raised with impurities infiltration angle factor decreased. Accordingly melt fluxing is effective method for achieving high undercooling of melt and formation of bulk amorphous alloys.

2) When undercooled Pd₈₂Si₁₈ melts are undercooled below 190 K, liquid phase separation (LPS) of undercooled melt will take place. LPS will provide higher driving force for crystallization of undercooled melts. Thus its glass forming ability is decreased. If the undercooled Pd₈₂Si₁₈ melts are transformed to amorphous alloy, it must stride over LPS regions.

3) Compared with amorphous ribbons prepared by melt spinning, exothermic peaks of DSC curve in bulk Pd₈₂Si₁₈ amorphous alloy change from one to two. It may be explained that bulk amorphous alloys compose of two amorphous parts with different composition or "structure", while amorphous ribbons with higher disorder state. The distinction can be ascribed to the links of between cooling rates of undercooled melt and crystallization of Pd₈₂Si₁₈ amorphous alloys.

4) When compared to rapidly quenched glassy Pd₈₂Si₁₈ ribbons, the present glass transition temperature T_g , crystallization temperature T_x , region of undercooling liquid ($\Delta T = T_x - T_g$) of bulk glassy Pd₈₂Si₁₈ alloys have been changed. Experimental results show that purifying melt may not only enhance glass forming ability (GFA) of undercooled melt but also improve thermal stability of the amorphous alloys.

REFERENCES

- [1] Busch R. Thermodynamics and kinetics of Zr-Ti-Cu-Ni-Be bulk metallic glass forming liquids[J]. *Materials Science and Engineering A*, 2000, 304 - 306(1- 2): 97 - 102.
- [2] Nishiyama N, Matsushita M, Inoue A. Crystallization and glass forming ability of supercooled Pd-Cu-Ni-P melt [J]. *Materials Transactions*, 2001, 42(6): 1068 - 1073.
- [3] Perepezko J H, Smith J S. Glass formation and crystallization in highly undercooled Ti-Cu alloys[J]. *Journal of Non-Crystalline Solids*, 1981, 44(1): 65 - 83.
- [4] Kui H W, Greer A L, Turnbull D. Formation of bulk metallic glass by fluxing[J]. *Applied Physics Letters*, 1984, 45(6): 615 - 616.
- [5] Lau C F, Kui H W. Critical cooling rate of amorphous Pd₄₀Ni₄₀P₂₀[J]. *Journal of Applied Physics*, 1993, 73 (5): 2599.
- [6] Guo W H, Kui H W. Formation of bulk nanostructured materials by rapid solidification[J]. *J Mater Res*, 2000, 15(7): 1606 - 1611.
- [7] Chou C, Peter P, Turnbull D. Transformation behavior of Pd-Au-Si metallic glass[J]. *Journal of Non-Crystalline Solids*, 1975, 17(2): 169 - 188.
- [8] Uhlmann D R. Kinetic treatment of glass formation[J]. *Journal of Non-Crystalline Solids*, 1972, 7(4): 337 - 348.
- [9] Tsang K H, Kui H W. Viscosity of molten Pd₈₂Si₁₈ and the scaling of viscosities of glass forming systems[J]. *J Appl Phys*, 1992, 72(1): 2599 - 2601.
- [10] Lee K L, Kui H W. Phase separation in undercooled molten Pd₈₀Si₂₀: Part I [J]. *J Mater Res*, 1999, 14 (9): 3653 - 3662.
- [11] Gangopadhyay A K, Croat T K, Kelton K F. The effect of phase separation on subsequent crystallization in Al₈₈Gd₆La₂Ni₄[J]. *Acta Mater*, 2000, 48(16): 4035 - 4043.
- [12] GUO Wen-hua. Formation of Bulk Nanostructure Materials: Ph. D. Thesis[M]. Hong Kong: The Chinese University of Hong Kong Library, 1998.
- [13] Masumoto A, Maddin R. Structural stability and Mechanical properties of amorphous metals[J]. *Materials Science and Engineering*, 1975, 19: 1 - 24.
- [14] Calka A, Radlinski A P. DSC study of surface induced crystallization in Pd-Si metallic glass[J]. *Acta Metall*, 1987, 35(7): 1823 - 1829.
- [15] Chen H S. Thermodynamic considerations on the formation and stability of metallic glass[J]. *Acta Metall*, 1974, 22(12): 1505 - 1511.
- [16] Keiton K F. Study of the devitrification of Pd₈₂Si₁₈ over a wide temperature range[J]. *Acta Metallurgica*, 1985, 33(3): 455 - 464.

(Edited by HE Xue-feng)